Coastal Dynamics 2017
Paper No. 055

IMPACTS OF SEASONAL FORCINGS ON THE HYDRODYNAMICS OF OREGON INLET, NC

Liliana Velásquez Montoya[1] and Margery F. Overton[1]

Abstract

This study explores the hydrodynamic response of a tidal inlet to wave climate seasonality by means of a process based numerical model. We assess the model performance relative to water levels and waves measured at nearby gauges. The validated model is used to study the spatial and temporal changes in the hydrodynamics within the inlet and in its area of influence. Seasonal changes in the circulation patterns through the inlet are analyzed with respect to their implications for seasonal morphology. The results from this study serve to illustrate the dynamicity of a wave-dominated tidal inlet and the spatio-temporal variability of waves' effects on inlet hydrodynamics. Studies of this kind provide information to face challenges on infrastructure design and to plan for strategic navigation and inlet management practices.

Key words: wave seasonality, Outer Banks, numerical modeling, Delft3D, semi-permanent inlets, tidal inlet circulation.

1. Introduction

Tidal inlets are strategic locations for navigation, recreation and fisheries. They regulate the exchange of water, pollutants, nutrients, and sediments between lagoons and oceans. Understanding the circulation and responses of tidal inlets to changing natural forces is therefore of utmost interest to manage these dynamic features and the infrastructure in their areas of influence. Hydrodynamics of tidal inlets have been explained at length by Bruun (1978); Mehta and Joshi (1988); Van De Kreeke (1988), among others. Advances in numerical modeling have allowed studies to investigate wave effects on tidal inlets' circulation and closure mechanisms (Bertin et al., 2009; Dodet et al., 2013; Olabarrieta et al., 2011; Ranasinghe and Pattiaratchi, 1999). Still, further investigations are required to enhance the understanding of wave effects on seasonal dynamics at semi-permanent inlets in large estuaries.

This paper presents the seasonal hydrodynamics of a tidal inlet that has remained open over 170 years in the Outer Banks of North Carolina, USA. Oregon Inlet has been subject of multiple studies regarding the design of a dual jetty system (Jarrett, 1978; Vemulakonda et al., 1985) that has not been built, and the construction of a terminal groin in its down drift side (Joyner et al., 1998; Miller et al., 1996; Overton et al., 1992). These studies provide a general understanding of the dynamics of Oregon Inlet, but their outcomes are restricted by the spatial and temporal resolution of monitoring efforts in the region and the scarcity of hydrodynamic measurements near the inlet.

Our aim is to enhance the knowledge of Oregon Inlet at spatial (meters) and temporal (tidal cycle, tidal month and seasons) scales that have not been investigated before. This study explores the hydrodynamic response of the inlet to changes in wave climate by means of a process-based numerical model that allowed us to identify the spatial extent of wave effects in the inlet. Results include circulation patterns for calm and energetic wave conditions and analysis of their implications for the morphological evolution of the inlet. The results of this study provide useful information to face challenges on inlet management practices, navigation, and infrastructure design in Oregon Inlet. Moreover, the validated hydrodynamic model presented here will be used in future work as the basis of a morphological model that will be used to investigate the evolution of the inlet and its interaction with a storm-induced ephemeral inlet that opened 10 km to the south of Oregon Inlet in 2011.

[1] North Carolina State University, Raleigh, NC, USA. lvelasq@ncsu.edu, overton@ncsu.edu

2. Study Area

Oregon Inlet is located in the Outer Banks of North Carolina, a wave-dominated barrier island system between the Atlantic Ocean and the Albemarle-Pamlico Sound (Figure 1). Oregon Inlet opened in 1846 during a storm and by 1989 had migrated approximately 3.5 km southward and 0.6 km landward (Joyner et al., 1998). Today, the northern spit located in Bodie Island remains responsive to littoral drift processes, while the south side of the inlet is stable because of a terminal groin completed in 1991 to protect the abutment of the Herbert C. Bonner Bridge crossing the inlet. The migratory nature of the Oregon Inlet generates an asymmetric geometry in which the main channel is in the southernmost space between the northern spit and the terminal groin with depths up to 14 m and minimum widths ranging from 630 m to 1,000 m (Figure 1).

The mean tidal ranges of the two closest gauge stations to Oregon Inlet are 0.98 m in the ocean side at the U.S. Army Corps of Engineers (USACE) Field Research Facility (FRF) and 0.28 m in the sound side at Oregon Inlet Marina (Figure 1). The wave climate in the region is characterized by two seasons; during the winter (October to April), extratropical storms generate northeasterly waves with significant wave heights (Hs) that vary between 2 and 5 m at 17 m depth. During the summer (May to September), waves with Hs of less than 1 m arrive to the vicinity of the inlet from the east-southeast (see seasonal wave roses in Figure 1). The calm conditions of the summer are occasionally disrupted by the occurrence of tropical storms during the hurricane season (June to November). All the aforementioned conditions result in a longshore transport rate near the inlet of about 700,000 m^3/yr to the south (Inman and Dolan, 1989; Jarrett, 1978).

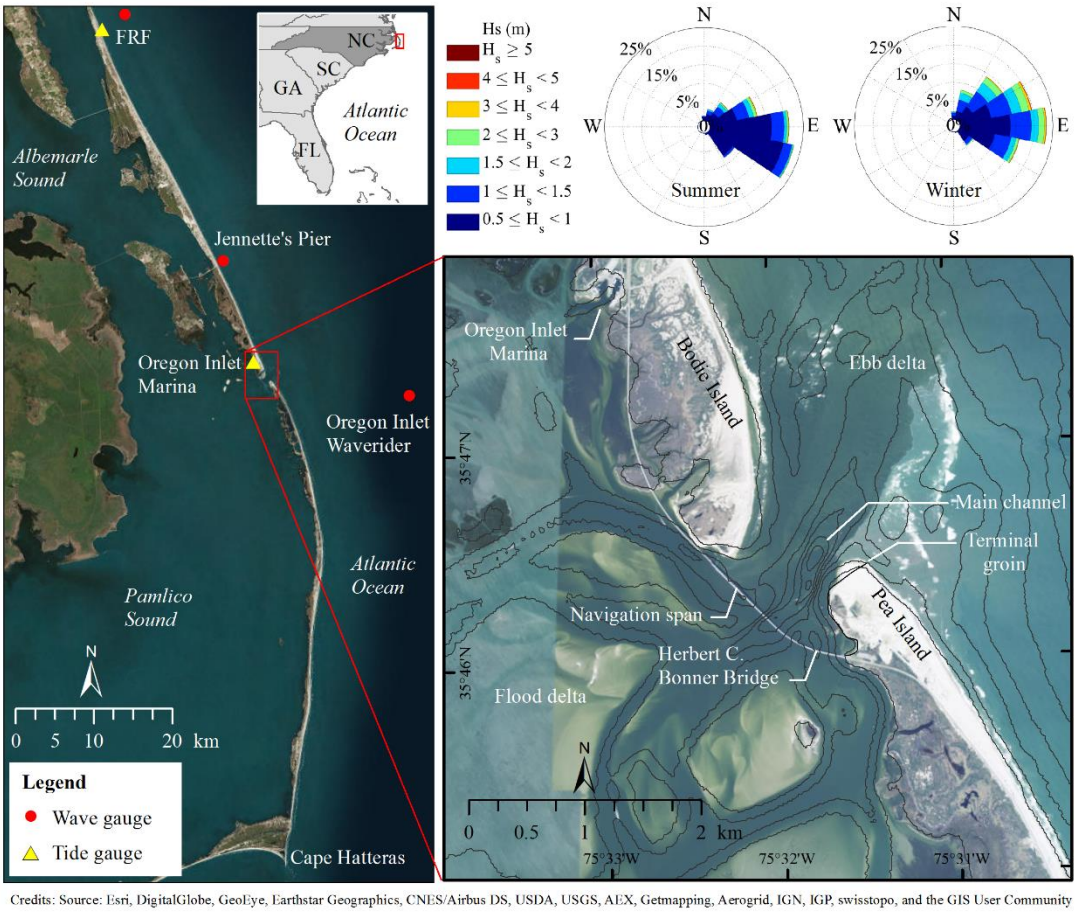

Credits: Source: Esri, DigitalGlobe, GeoEye, Earthstar Geographics, CNES/Airbus DS, USDA, USGS, AEX, Getmapping, Aerogrid, IGN, IGP, swisstopo, and the GIS User Community

Figure 1. Location of Oregon Inlet and seasonal wave roses created from data recorded at the FRF from 1997 to 2015.

3. Data and Methods

Data used in this study include information to support grid design and to define the spatial domain of the hydrodynamic model for Oregon Inlet, such as aerial photography and shorelines. We also required forcings to use as boundary conditions for the model (i.e. bathymetry, water levels, waves, winds) and data to evaluate the model performance, such as available records of hydrodynamic variables near Oregon Inlet. Section 3.1 presents the data sources, their location and resolution. The hydrodynamic model used to study Oregon Inlet is explained in detail in section 3.2.

3.1 *Observations of waves, tides, and wind*

Wave and tidal records are available at the gauges shown in Figure 1. The longest wave record near Oregon Inlet is available from the FRF gauge at 17 m depth; this station provides Hs, wave direction (Dir) and peak period (Tp) every 30 minutes from 1997 to present. The data of this station helped to identify the seasonal wave climate in the region. Oregon Inlet Waverider is a wave gauge located at 18 m depth seaward of Oregon Inlet (Figure 1). This station is owned by the Coastal Studies Institute and was active from 2012 to 2016, the wave boundary conditions used to force the model in this study come from this station. Jennette's Pier and Oregon Inlet Marina are the only wave and tide gauges within the model domain (Figure 1 and 2). Wave records in the former station are available from September 2012 to March 2014 at 11 m depth, while the latter has been measuring hourly water levels from 1996 and wind conditions from 2007 to present. Data from these two stations was used to evaluate the model performance. Table 1 presents a summary of the data available in each gauge and its usage in this study.

Table 1. Gauges and data availability in the study area.

Name	Measured variables	Time frame available	Usage
FRF 17 m depth	Waves (Hs, Tp, Dir)	1997 - present	Seasonal wave climate
Oregon Inlet Waverider	Waves (Hs, Tp, Dir)	2012 - 2016	Boundary conditions
Jennette's Pier	Waves (Hs, Tp, Dir)	Sept. 2012 - Mar. 2014	Model Evaluation
Oregon Inlet Marina	Water levels	1996 - present	Model Evaluation
	Wind	2007 - present	Boundary conditions

3.2 *Hydrodynamic and Wave Models of Oregon Inlet*

The hydrodynamic and online wave-coupled model of Oregon Inlet is based on the modeling platform Delft3D (Lesser et al., 2004), which has been used to simulate tidal inlet hydrodynamics by Castelle et al. (2007); Elias et al. (2006); Sennes et al. (2007). This software suite has built-in coupling of multiple modules, among those, we use the FLOW and WAVE. The hydrodynamic model (FLOW) solves the two-dimensional depth-averaged (2DH) continuity equation and horizontal momentum equations, while the vertical momentum equation is reduced to the hydrostatic pressure relation by assuming gravity to be the major vertical acceleration. The WAVE module uses the third generation Simulating WAves Nearshore (SWAN) model (Booij et al., 1999) that solves the spectral action balance equation. SWAN accounts for refractive wave propagation due to currents and depth and represents wave generation by wind, dissipation due to whitecapping, bottom friction, depth-induced wave breaking, and non-linear wave-wave interactions. Deltares (2014a, 2014b) explain all mathematical formulations and equations solved in both modules of Delft3D in detail.

Delft3D uses a finite difference scheme to solve the system of partial differential equations. The region surrounding Oregon Inlet was discretized in two curvilinear grids with increasing resolution near the inlet (Figure 2b), both grids communicate with one another through internal boundaries. The external grid has 12,764 elements and the internal grid has 34,776 elements, with edge lengths that range between 14 m in Oregon Inlet and 460 m near the boundaries (Table 2). The wave grid has 18,213 elements and extends far offshore and alongshore to prevent any boundary problems from propagating into the hydrodynamic grid. During the computation, SWAN obtains current information by bilinear interpolation from the

hydrodynamic grid. The intra-model communication happens every 20 minutes, and the hydrodynamic time step is 30 s.

Table 2. Delft3D grids characteristics.

Grid	Number of elements	Minimum element size (m)	Maximum element size (m)
External	12,764	45	461
Internal	34,776	14	223
Wave	18,213	43	788

To schematize as accurately as possible the bottom in different regions of the domain, the bathymetry of the model was generated by merging multiple sources of topo-bathymetric data. Depths in the Croatan Sound (northwest sound) are based on the 2002 NOAA sounding; the flood delta of Oregon Inlet and the topography near the inlet are based on the 2014 Post Sandy Topo-Bathy Lidar; the depths in the main channel of the inlet were obtained from the hydrographic survey of Oregon Inlet by the USACE on April 2014. Elevations and depths for the rest of the model domain are based on the digital elevation model of the flood mapping program of the Federal Emergency Management Agency (FEMA) (Blanton et al., 2008). The final bathymetry is a composite of the most recent topo-bathymetric data in the region, given the multi-temporal nature of the data, the bathymetry does not represent an instantaneous state of the inlet, instead it captures its most important features creating a realistic model of the bottom. Oregon Inlet is represented with a well-defined main channel, a complex set of sinuous channels in the flood delta and the steep edge of the ebb delta in the ocean side (Figure 2c), locations of all features match those visible from orthophotos and satellite images of the inlet.

The model includes the two main structures in the study area. The Herbert C. Bonner Bridge is schematized as a porous plate with a loss coefficient of 0.44 dependent on the blocking of the flow by the bridge piers (Farraday and Charlton, 1983). The loss coefficient is used to determine the additional quadratic friction term in the momentum equation. The terminal groin is schematized as thin dam, which is an infinitely thin object used in Delft3D to represent flow obstacles in the model that prohibit flow exchange between adjacent cells.

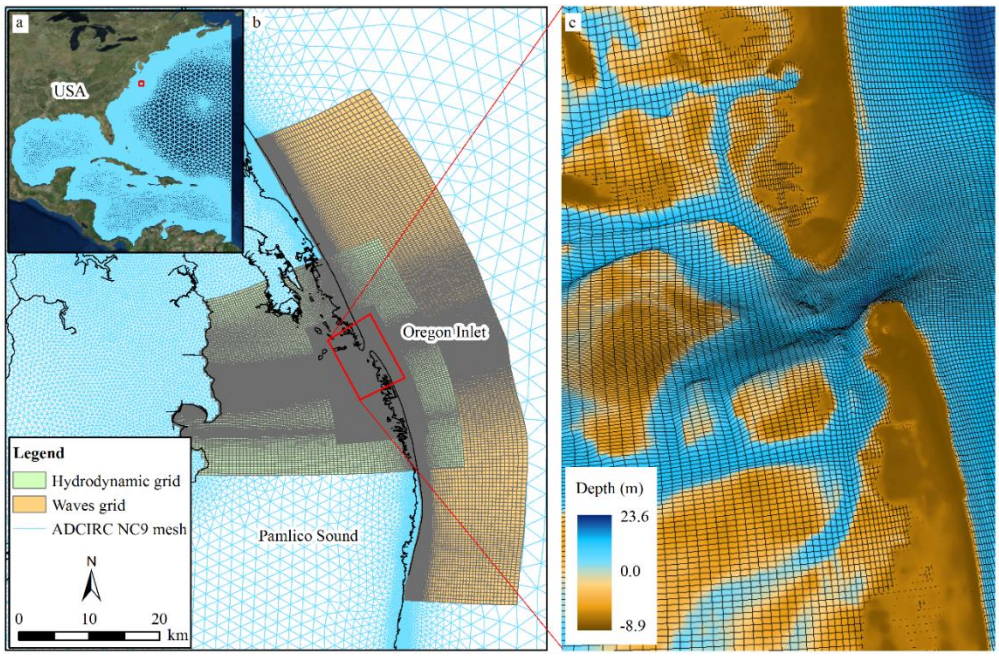

Figure 2. Model domain. a) ADCIRC NC9 Mesh for the Western North Atlantic Ocean; b) Delft 3D FLOW and WAVE grids; c) Grid and bathymetry near Oregon Inlet (negative depth values indicate elevation above 0 m NAVD 88).

The shoreline of mainland North Carolina forms the closed boundary on the west side of the model. In the lateral (north and south) and open-ocean (east) boundaries, water levels are fed from simulations of the ADvanced CIRCulation model for oceanic, coastal and estuarine water (ADCIRC) (Luettich et al., 1992; Westerink et al., 2008). ADCIRC was run using the high resolution mesh for the coast of North Carolina (NC9 mesh) and forced by 8 tidal constituents (M2, S2, N2, K2, K1, O1, P1 and Q1) in the open-ocean boundary and wind forcing from the ADCIRC Surge Guidance System (Dresback et al., 2013). Figure 2a and b show the ADCIRC mesh relative to the Delft3D grids of Oregon Inlet. Wave conditions are extracted from Oregon Inlet Waverider and are assumed to remain spatially constant along the open-ocean boundary of the wave model.

Each simulation starts from a uniform water level, followed by a 15-day spin-up period of tide-only forcing. After this period, the model dissipates the errors from the transition between its initial state and that imposed by the boundary conditions. Calibration and validation simulations forced by tides and waves were run over fortnight periods that include a spring and neap tidal cycle, which are considered to provide sufficient conditions to evaluate the model performance.

4. Results

4.1 *Model calibration*

Multiple simulations were set up to test model stability with different time steps, processes and simplified boundary conditions. Once the model showed a stable behavior, the calibration of the physical parameters of the model began. The calibration period is January 4 – 19, 2014; this period was selected because of the availability of data to force the models (ADCIRC and Delft3D) and because of continuous records of water levels and wave conditions at Oregon Inlet Marina and Jennette's Pier were available to compare with the model results. The evaluation of the model was done statistically by computing the Mean Absolute Error (MAE) as defined in Sutherland et al. (2004) and by visually comparing simulated and observed water levels and waves at the aforementioned stations.

Effects of boundary conditions on the model performance were tested by running simulations with two ADCIRC meshes with varying resolution near the inlet (NC6B and NC9). As expected, the best results were obtained when using water levels from the high-resolution ADCIRC mesh for North Carolina (NC9) to force the Delft3D model of Oregon Inlet. The two physical parameters calibrated for the model were the bed roughness and the horizontal eddy viscosity. Both parameters were varied within a range of acceptable values for coastal settings (Table 3) and their final values were chosen as the combination resulting in the most accurate simulation of water levels and waves at Oregon Inlet Marina and Jennette's Pier respectively. Given that there are not current measurements available in the inlet, the model was verified to reach flow velocities close to those reported in the literature.

Table 3. Range of parameters and sources of water level boundary conditions tested for model calibration. Bold values are the final calibrated settings.

Parameter	Evaluation range
Bed roughness coefficient	**Chezy: 65** Manning: 0.018, 0.02, 0.024
Horizontal eddy viscosity (m^2/s)	**1**, 10, 50, 100
Source of water level boundary conditions (mesh resolution near Oregon Inlet)	ADCIRC NC6B mesh (110 m) **ADCIRC NC9 mesh (25 m)** ADCIRC NC9 mesh for open-ocean and Newmann lateral boundaries

Under this evaluation method, the simulated water levels that had the best match with measurements at Oregon Inlet Marina were obtained from a simulation with a Chezy coefficient and horizontal eddy viscosity of 65 and 100 m^2/s respectively. Such simulation had a MAE of 0.06 m for water levels. Nevertheless, we found that under these settings, the mean velocity within the inlet was 0.6 m/s and it never exceeded 1.3 m/s. Such velocities are relatively low compared to those reported by Nichols and Pietrafesa (1997), who state that Oregon Inlet mean flow velocity is about 0.9 m/s and those measured in 2011 by Ocean Engineering International (2012), who captured velocities of up to 2.6 m/s across the inlet. Revision of the parameters lead to their final values shown in bold in Table 3, which correspond to the default values in Delft3D and resulted in a MAE of 0.07 m for water levels and 0.29 m for Hs. These values led to more realistic velocities in the inlet than the previous set of parameters, this improvement was obtained at the expense of a slight decrease in tidal signal accuracy at Oregon Inlet Marina (Figure 3a).

The left panels in Figure 3 show the comparison of observed and simulated water levels at Oregon Inlet Marina (a) and wave conditions at Jennette's Pier (b to d) for the calibration period. Simulated water levels follow the general tidal signal at the marina; nevertheless, the model fails to reproduce 50% of the peaks and troughs of the tidal record. This inaccuracy of model can be explained because of the protected location of the tidal gauge and the lack of detail in the bathymetry in its vicinity. Simulated waves reproduced the observed wave conditions closely, with a few exceptions. Discrepancies between the model and the observations can be explained by temporary changes in wind/sea conditions that may not have been present in the forcings of the model at those specific instants of time.

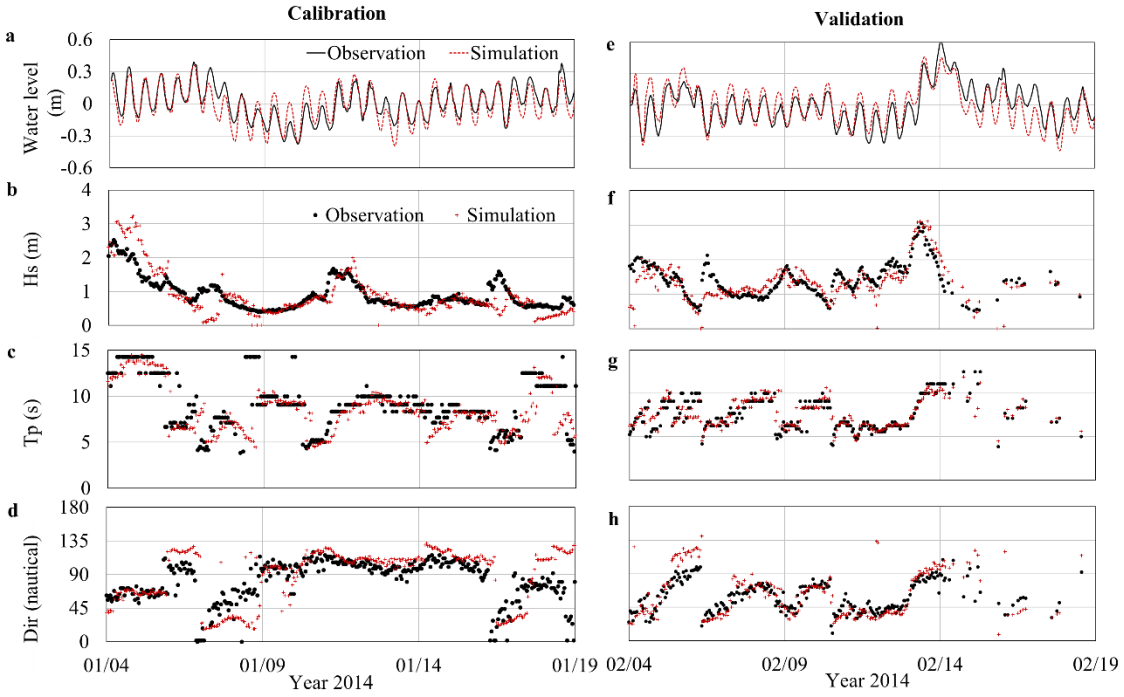

Figure 3. Comparison of time series of observed and simulated water levels at Oregon Inlet Marina (a, e); significant wave height (b, f), peak period (c, g) and nautical wave direction (d, h) at Jennette's Pier for the calibration (left) and validation (right) fortnight periods.

4.2 *Model validation*

The validation period goes from February 4 to 19, 2014. Availability of data to force and evaluate the model led to the selection of this fortnight period, which also includes a storm that generated 3 m Hs in Jennette's Pier and a surge of 0.6 m in Oregon Inlet Marina. The model showed a similar behavior as that of the calibration period. Simulated water levels in Oregon Inlet Marina follow the observations (Figure 3e), but the model usually over predicted the tidal peaks. The model does a good job capturing the growth

rate, duration and decay of the surge that occurred between February 13 and 15, but it under predicted its peak by 0.1 m. Regarding simulation of wave conditions, the model captures most of the observed Hs, Tp and Dir including abrupt changes in direction and temporal variation on heights and periods for calm and energetic conditions (Figure 3f - h).

The MAE for water levels and Hs is 0.11 m and 0.29 m respectively. These errors are of the same order of magnitude as those from the calibration period. Possible causes of those errors are missing details in the bathymetry caused by merging multiple surveys near the inlet. In particular, the location of Oregon Inlet Marina poses a big challenge for model evaluation given the unchartered waters in its vicinity. Nevertheless, the model shows consistency to predict water levels in the sound, waves in the ocean side and flow velocities in the inlet that fall within the reported currents' magnitude. This behavior provides confidence in the hydrodynamic model to study the effects of seasonal forcings in Oregon Inlet dynamics.

4.3 *Seasonality of Oregon Inlet*

To identify the impact of wave seasonality in Oregon Inlet dynamics, two simulations forced with representative wave conditions of the summer and the winter were developed. The two simulations were hot-started from a tide-only run, each simulation lasted a month, and both are forced with equal tidal conditions extracted from the Western North Atlantic ADCIRC Tidal Database (Westerink et al., 1993). Wave boundary conditions correspond to observed waves at Oregon Inlet Waverider for January 2013 (winter) and July 2012 (summer). These specific months were chosen because they include wave conditions that follow the general patterns expected for each season (Figure 3). The winter month includes four events with Hs higher than 2 m (gray bands in Figure 3), three of them with waves predominantly from the north-northeast and the last one with waves from the south-southeast. In the summer, waves primarily from the south and southeast remained below 2 m. These boundary conditions allowed us identifying the hydrodynamic responses of the inlet to the two contrasting periods. Model outputs were analyzed at low, high and higher high tide for the period of time marked with the darkest gray background in Figure 3, which coincides with spring tide.

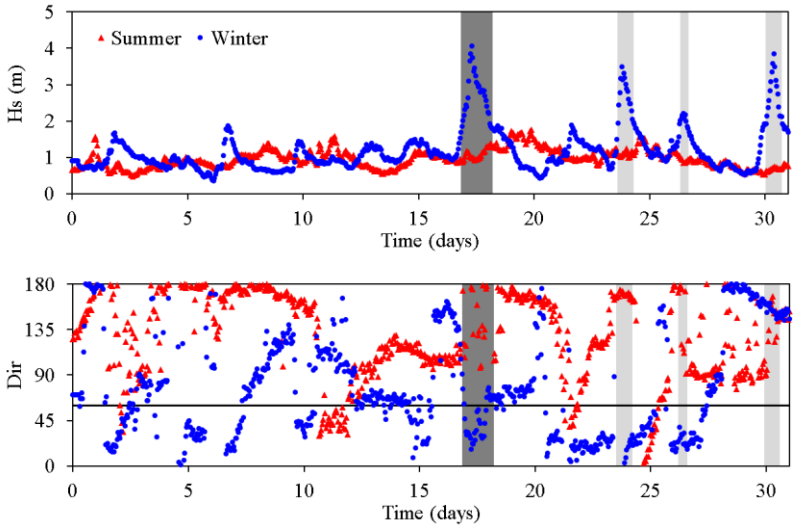

Figure 3. Wave boundary conditions from Oregon Inlet Waverider at 18 m depth. Top: Time series of significant wave heights. Bottom: Time series of nautical wave direction.

Figure 4 shows the depth-averaged velocities in Oregon Inlet at different stages of the tidal cycle (columns) and times when wave conditions represent two different seasons (rows). At low tide (first column), the ebb current flows from the sinuous channels of the flood delta in the sound, through the inlet main channel closer to the terminal groin, and reaches the ocean. In the summer, the main ebb current is unidirectional, heading northeast with depth-averaged velocities up to 1.2 m/s (Figure 4a). Under energetic

waves from the northeast (Figure 4b), wave-induced currents in the ocean rotate the ebb current 3° southward. A north-south longshore current develops at both sides of the inlet generating a residual flood current in the north bank of the inlet that constricts the main ebb current. This longshore current continues flowing to the south past the pocket of the terminal groin, which is located in the shadow zone of the ebb current.

During high tide, the flood current flows through all the extent of the inlet, the water in the ocean side is funneled into the sound and distributed among the channels in the flood delta. This pattern is similar for summer and winter conditions. The highest velocities under these forcings occur near the tip of the terminal groin directed towards the inlet (Figure 4c and d). This current could be one of the causes of the sporadic formation of a sand spit in the south side of the inlet, like the one visible in Figure 1. During the summer, there is not a well-defined longshore current, while during energetic conditions it can reach about 0.75 m/s flowing north to south until it merges with the flood current entering the inlet. The southward longshore current reestablishes 1.5 km south of the terminal groin (Figure 4d).

At higher high tide, the flood current reaches velocities of 2 m/s (Figure 4e and f). Similar to the previously described circulation pattern, the water enters through the inlet for calm and energetic conditions. A significant change in the circulation occurred in the ocean side, where the model captures a reversal of the longshore current. In the previous energetic scenarios, waves approached the inlet from the northeast, but in this case, waves come from the east-northeast, which causes the longshore current to flow from south to north. This longshore current reversal has been reported by Miller et al. (1996), who found that significant net potential sediment transport toward the north could occur near Oregon Inlet.

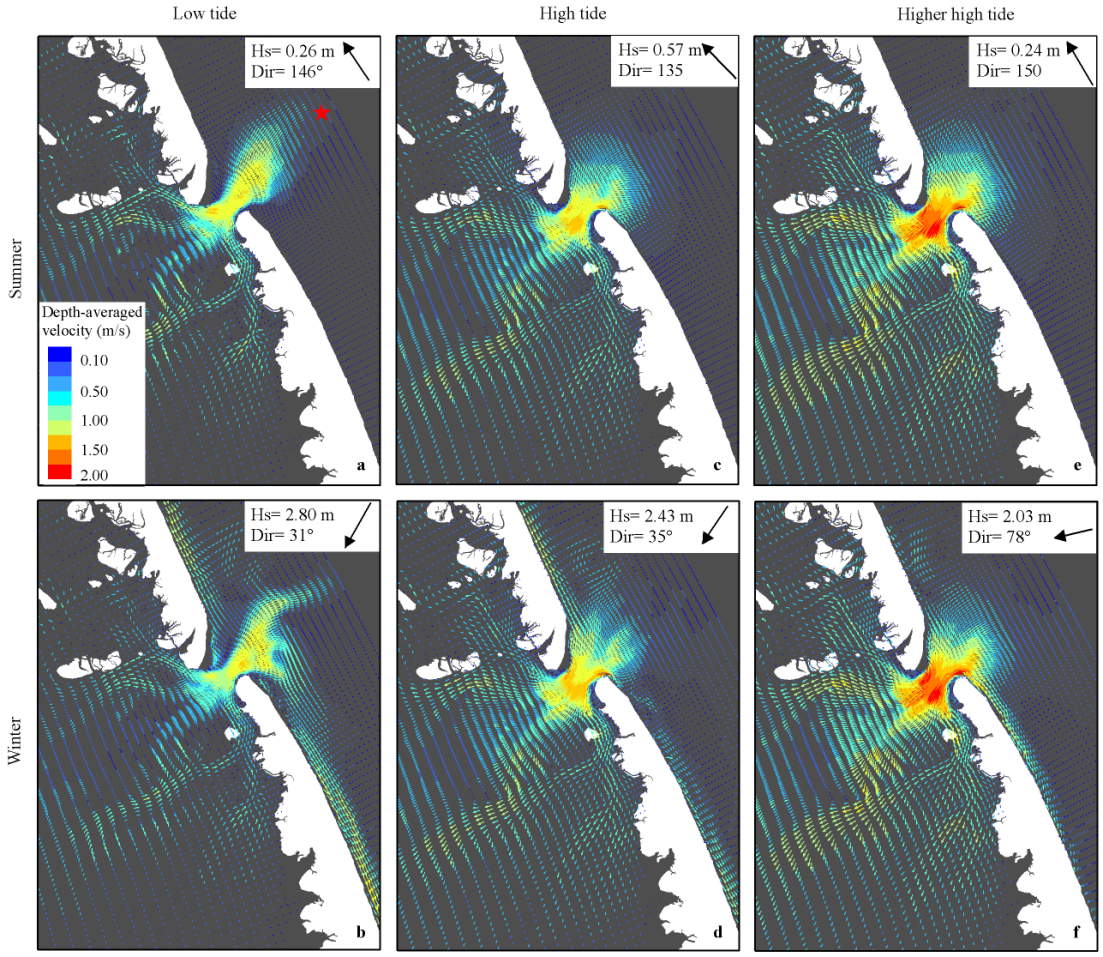

Figure 4. Seasonal circulation in Oregon Inlet. Wave conditions in the white boxes correspond to those simulated at 15 m depth at the location marked with a red star in the top left panel.

After reviewing the model outputs at different times and with varying wave conditions, we found that the longshore current shifts when waves travel from directions higher than 60°. When waves approach north of this direction, the resulting longshore current matches the predominant southward littoral drift. In the wave records used to force the seasonal simulations, 75% of the waves approached the inlet from directions between 60° and 180° (markers above the black line on the bottom panel of Figure 3), but waves with these directions were usually not high enough to create northward longshore currents faster than 0.05 m/s. From the four high-energy events simulated, only the last one had all waves coming from the southeast. These results suggest that despite the predominant littoral drift travels toward the south, reverse periods can occur more often than previously thought, especially when tropical storms travel offshore towards the North Carolina coast, which results in swells traveling south to north.

The spatial extent and variation of wave effects are expected to influence not only the hydrodynamics of the system, but also its morphology. An initial overview of the spatial variability of those effects, is presented in Figure 5, which includes the 0.2 N/m^2 bed shear stress contours at low (left), high (center) and higher high tide (right) for summer and winter conditions. A 0.2 N/m^2 bed shear stress is considered the minimum critical shear stress for initiation of motion for sands with d_{50}= 200 μm (van Rijn, 2007), thus this contour provides an idea of the nearshore regions where active sediment transport takes place near Oregon Inlet, which has sediment sizes of the order of 220 μm (Dolan et al., 2003).

The most important differences in the spatial distribution of bed shear stresses between summer and winter occur in the ocean side, where winter waves have effects on the bottom farther offshore along the coast and the edge of the ebb delta than summer waves (Figure 5). In the sound side, the spatial distribution of the bed shear stress is highly dependent on the tidal flow rather than the wave conditions. During low tide, the bed shear stresses that could rework sediments are located within the sinuous channels of the flood delta (Figure 5 left), while at high tide, the 0.2 N/m^2 contour covers most of the flood delta (Figure 5 center and right). This pattern indicates that ebb currents shape the channels in the sound, while flood currents are distributed across the whole flood delta generating higher bed shear stresses in the shoals where ebb currents do not have major effects on the bottom.

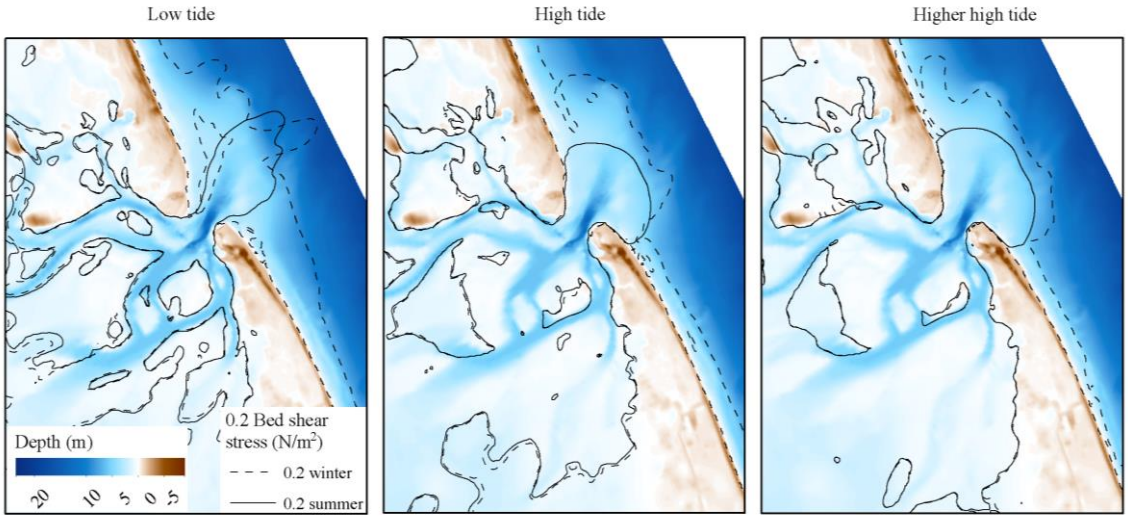

Figure 5. Bed shear stress 0.2 N/m^2 contour for summer and winter at different stages of the tidal cycle.

5. Conclusion and Future Work

A coupled hydrodynamic and wave model was calibrated and validated for Oregon Inlet using observed tides and waves in the sound and ocean, respectively. The model allowed us to identify the following circulation patterns of the inlet under summer and winter forcings. During the summer, tidal flow regulates the hydrodynamics of the inlet. The high-energy waves of the winter rotate the ebb current southwards and

generate longshore currents in the same direction that can reach velocities of 0.75 m/s. Waves coming south of 60° reverse this longshore current, generating a flow in the opposite direction of the dominant littoral drift near Oregon Inlet. This longshore current could be one of the factors leading to sand accumulation adjacent to the terminal groin in the down drift side of the inlet. Ebb currents drain through the channels in the flood delta while flood currents enter the sound inundating most of the flood delta and shaping the shoals.

A morphological model based on the validated hydrodynamic model presented here is under development. Recent evaluation of the morphological behavior of the model indicates that it can capture general erosional and depositional trends within the Oregon Inlet. Future work to study the response of the inlet to natural processes and structures will couple model outputs with multi-temporal geospatial analysis of the main morphological features of the inlet (e.g. northern spit, shoals).

Acknowledgements

We would like to thank Dr. Casey Dietrich for his advice and cooperation to set up ADCIRC simulations in the high-resolution mesh for North Carolina and Dr. Brian Blanton from the Renaissance Computing Institute from providing access to the ADCIRC repositories from the Coastal Emergency Risks Assessment. The authors are also grateful to the NOAA's Center for Operational Oceanographic Products and Services (CO-OPS) and the U.S. Army Engineer Research & Development Center, Coastal & Hydraulics Laboratory, Field Research Facility, Duck, North Carolina for making available the observational datasets used in this study.

References

Bertin, X., Fortunato, A.B., Oliveira, A., 2009. A Modeling-based Analysis of Processes Driving Wave-dominated Inlets. *Continental Shelf Research*, 29, 819–834.

Blanton, B., Madry, S., Galluppi, K., Gamiel, K., Lander, H., Reed, M., Stillwell, L., Blanchard-Montgomery, M., 2008. *Report for the State of North Carolina Floodplain Mapping Project: Coastal Flood Analysis System. Topographic/Bathymetric Data*.

Booij, N., Ris, R.C., Holthuijsen, L.H., 1999. A Third-generation Wave Model for Coastal Regions: 1. Model Description and Validation. *Journal of Geophysical Research*, 104, 7649–7666.

Bruun, P., 1978. Stability of Tidal Inlets. *Theory and Engineering*. Elsevier Scientific Publishing Company, Trondheim, Norway.

Castelle, B., Bourget, J., Molnar, N., Strauss, D., Deschamps, S., Tomlinson, R., 2007. Dynamics of a Wave-dominated Tidal Inlet and Influence on Adjacent Beaches, Currumbin Creek, Gold Coast, Australia. *Coastal Engineering*. 54, 77–90.

Deltares, 2014a. Delft3D - *FLOW. Simulation of Multi-dimensional Hydrodynamic Flows and Transport Phenomena, Including Sediments. User Manual*. Deltares, Delft, the Netherlands.

Deltares, 2014b. Delft3D WAVE. *Simulation of short-crested waves with SWAN. User Manual*. Deltares, Delft, the Netherlands.

Dodet, G., Bertin, X., Bruneau, N., Fortunato, A.B., Nahon, A., Roland, A., 2013. Wave-Current Interactions in a Wave-Dominated Tidal Inlet. *Journal of Geophysical Research*. Ocean. 118, 1587–1605.

Dolan, R., Smith, J., Dofflemeyer, S., Sims, C., 2003. *Compatibility Study of Sand Bypassing from Oregon Inlet to Pea Island National Wildlife Refuge (North Carolina)*. Charlottesville, VA.

Dresback, K.M., Fleming, J.G., Blanton, B.O., Kaiser, C., Gourley, J.J., Tromble, E.M., Luettich, R.A., Kolar, R.L., Hong, Y., Van Cooten, S., Vergara, H.J., Flamig, Z.L., Lander, H.M., Kelleher, K.E., Nemunaitis-Monroe, K.L., 2013. Skill Assessment of a Real-time Forecast System Utilizing a Coupled Hydrologic and Coastal Hydrodynamic Model during Hurricane Irene (2011). *Continental Shelf Research*. 71, 78–94.

Elias, E.P.L., Cleveringa, J., Buijsman, M.C., Roelvink, J.A., Stive, M.J.F., 2006. Field and Model Data Analysis of Sand Transport Patterns in Texel Tidal Inlet (the Netherlands). *Coastal Engineering*. 53, 505–529.

Farraday, R. V., Charlton, F.G., 1983. *Hydraulic Factors in Bridge Design*. Wallingford, Oxfordshire, England.

Inman, D.L., Dolan, R., 1989. The Outer Banks of North Carolina: Budget of Sediment and Inlet Dynamics along a Migrating Barrier System. *Journal of Coastal Research*, 5, 193–237.

Jarrett, J.T., 1978. Coastal processes at Oregon Inlet, North Carolina, in: *16th International Conference on Coastal Engineering*. ASCE, Hamburg, Germany, pp. 1257–1275.

Joyner, B.P., Overton, M.F., Fisher, J.S., 1998. Post-Stabilization Morphology of Oregon Inlet, NC, in: *26th Conference in Coastal Engineering*. ASCE, Copenhagen, Denmark, pp. 3124–3137.

Lesser, G.R., Roelvink, J.A., van Kester, J.A.T.M., Stelling, G.S., 2004. Development and Validation of a Three-dimensional Morphological Model. *Coastal Engineering*, 51, 883–915.

Luettich, R.A., Westerink, J.J., Scheffner, N.W., 1992. *ADCIRC: an advanced three-dimensional circulation model for shelves coasts and estuaries, report 1: theory and methodology of ADCIRC-2DDI and ADCIRC-3DL*. Dredging Research Program Technical Report DRP-92-6. Vicksburg, MS.

Mehta, A.J., Joshi, P.B., 1988. Tidal Inlet Hydraulics. *Journal of Hydraulic Engineering*. 114, 1321–1338.

Miller, H.C., Dennis, W.A., Wutkowski, M.J., 1996. A Unique Look at Oregon Inlet, NC USA, in: *25th Conference on Coastal Engineering*. ASCE, Orlando, Florida, pp. 4517–4530.

Nichols, C.R., Pietrafesa, L.J., 1997. *Oregon inlet: Hydrodynamics, Volumetric Flux and Implications for Larval Fish Transport*. Raleigh, NC.

Ocean Engineering International, P., 2012. *B-2500, NC 12 - Replacement of Herbert C. Bonner Bridge across Oregon Inlet from Bodie Island to Hatteras Island, Dare County, NC*. Final Bridge Hydraulic Report. Gainesville, FL.

Olabarrieta, M., Warner, J.C., Kumar, N., 2011. Wave-Current Interaction in Willapa Bay. *Journal of Geophysical Research*, *Ocean*, 116, 1–27.

Overton, M.F., Fisher, J.S., Dennis, W.A., Miller, H.C., 1992. Shoreline change at Oregon Inlet terminal groin, in: *International Conference on Coastal Engineering*. ASCE, Venice, Italy, pp. 2332–2343.

Ranasinghe, R., Pattiaratchi, C., 1999. The Seasonal Closure of Tidal Inlets : Wilson Inlet — a Case Study. *Coastal Engineering*, 37, 37–56.

Sennes, G., Castelle, B., Bertin, X., Mirfenderesk, H., Tomlinson, R.B., 2007. Modelling of the Gold Coast Seaway Tidal Inlet, Australia, in: Proceedings of the 9th International Coastal Symposium. *Journal of Coastal Research*, Gold Coast, Australia, pp. 1086–1091.

Sutherland, J., Peet, A.H., Soulsby, R.L., 2004. Evaluating the Performance of Morphological Models. *Coastal Engineering*, 51, 917–939.

Van De Kreeke, J., 1988. Hydrodynamics of Tidal Inlets, in: Aubrey, D.G., Weishar, L. (Eds.), *Hydrodynamics and Sediment Dynamic of Tidal Inlets*. Springer-Verlag, New York.

van Rijn, L.C., 2007. Unified View of Sediment Transport by Currents and Waves. I: Initiation of Motion, Bed Roughness, and Bed-Load Transport. *Journal of Hydraulic Engineering*, 133, 649–667.

Vemulakonda, S.R., Swain, A., Houston, J.R., Farrar, P.D., Chou, L.W., 1985. *Coastal and inlet processes numerical modeling system for Oregon Inlet, North Carolina*. Vicksburg, Mississippi.

Westerink, J.J., Luettich, R.A., Feyen, J.C., Atkinson, J.H., Dawson, C., Roberts, H.J., Powell, M.D., Dunion, J.P., Kubatko, E.J., Pourtaheri, H., 2008. A basin- to channel-scale unstructured grid hurricane storm surge model applied to southern Louisiana. *Monthly Weather Review*, 136, 833–864.

Westerink, J.J., Luettich, R.A., Scheffner, N.W., 1993. *ADCIRC: An Advanced Three-dimensional Circulation Model for Shelves, Coasts, and Estuaries, Report 3: Development of a Tidal Constituent Database for the Western North Atlantic and the Gulf of Mexico*. Tech. Report DRP 92-6. Vicksburg, MS.